

Particle-Size Effects on Nuclear Magnetic Resonance in Superconductors*

FULTON WRIGHT, JR.†

Department of Physics, University of California, Berkeley, California

(Received 5 June 1967)

The Knight shift in the superconducting state has been observed in samples containing various sizes of small tin particles. The three main samples were constructed by vacuum evaporation of alternate layers of metal and dielectric (silicon monoxide). The particles are in the form of platelets whose diameter and thickness were measured with an electron microscope. The geometric means of the particle dimensions were 170, 300, and 570 Å. The fractions of the normal-state shift (referred to α tin) remaining at zero temperature were 84, 74, and 62%, respectively. Three other samples produced by a variety of processes gave results consistent with those of the main samples. The data fit well the theory of spin-reversing scattering through spin-orbit coupling which had been proposed to explain the nonzero Knight shift in superconductors. Two other possible contributions, a shift due to Van Vleck-type orbital susceptibility and crystalline-field spin-orbit coupling, cannot be ruled out theoretically, but do not appear to be important experimentally.

I. INTRODUCTION

IN the last ten years considerable effort, both experimental and theoretical, has been expended studying the Knight shift in superconductors.^{1-42a} This interest

was generated by the fact that the Bardeen, Cooper, and Schrieffer (BCS) theory of superconductivity,⁴³ when applied to the Knight shift problem,⁶ predicted that the shift would approach zero as the absolute temperature approached zero, whereas experiments indicated otherwise.^{3,16} Many possible explanations for the discrepancy between theory and experiment were proposed. One of the most promising of these was spin-reversing scattering through spin-orbit coupling.^{9,12} This mechanism predicted that the fraction of the Knight shift remaining at zero temperature in the superconducting state, $K(0)/K(T_c)$, would be a function of the size of the sample. Samples with at least

* Research supported in part by the U.S. Office of Naval Research.

† Present address: Education Research Center, Massachusetts Institute of Technology, Cambridge, Massachusetts.

¹ F. Reif, Phys. Rev. **102**, 1417 (1956).

² W. D. Knight, G. M. Androes, R. H. Hammond, Phys. Rev. **104**, 852 (1956).

³ F. Reif, Phys. Rev. **106**, 208 (1957).

⁴ F. Reif, in *Low Temperature Physics and Chemistry*, edited by J. R. Dillinger (The University of Wisconsin Press, Madison, 1958).

⁵ M. Tinkham, Phys. Rev. **110**, 26 (1958).

⁶ K. Yosida, Phys. Rev. **110**, 769 (1958).

⁷ V. Heine and A. B. Pippard, Phil. Mag. **3**, 1046 (1958).

⁸ G. M. Androes and W. D. Knight, Phys. Rev. Letters **2**, 386 (1959).

⁹ R. A. Ferrell, Phys. Rev. Letters **3**, 262 (1959).

¹⁰ P. C. Martin and L. P. Kadanoff, Phys. Rev. Letters **3**, 322 (1959).

¹¹ J. R. Schrieffer, Phys. Rev. Letters **3**, 323 (1959).

¹² P. W. Anderson, Phys. Rev. Letters **3**, 325 (1959).

¹³ J. C. Fisher, Australian J. Phys. **13**, 446 (1960).

¹⁴ Z. Galasiewicz, Progr. Theoret. Phys. (Kyoto) **23**, 197 (1960).

¹⁵ A. A. Abrikosov and L. P. Gor'kov, Zh. Exprim. i Teor. Fiz. **39**, 480 (1960) [English transl.: Soviet Phys.—JETP **12**, 337 (1961)].

¹⁶ G. M. Androes and W. D. Knight, Phys. Rev. **121**, 779 (1961).

¹⁷ L. E. Orgel, J. Phys. Chem. Solids **21**, 123 (1961).

¹⁸ J. Bardeen and J. R. Schrieffer, in *Progress in Low Temperature Physics*, edited by C. J. Gorter (North-Holland Publishing Company, Amsterdam, 1961), Vol. 3, p. 170.

¹⁹ R. Suzuki and M. Akano, Nuovo Cimento **21**, 559 (1961).

²⁰ H. Suhl, in *Low-Temperature Physics*, edited by C. De Witt, B. Dreyfus, and P. G. de Gennes (Gordon and Breach Publishers Inc., New York, 1962), p. 233.

²¹ L. N. Cooper, Phys. Rev. Letters **8**, 367 (1962).

²² A. M. Clogston, A. C. Gossard, V. Jaccarino, Y. Yafet, Phys. Rev. Letters **9**, 262 (1962).

²³ V. L. Ginzburg, Zh. Exprim. i Teor. Fiz. **41**, 828 (1961)

[English transl.: Soviet Phys.—JETP **14**, 594 (1962).]

²⁴ A. A. Abrikosov and L. P. Gor'kov, Zh. Exprim. i Teor. Fiz. **42**, 1088 (1962) [English transl.: Soviet Phys.—JETP **15**, 752 (1962).]

²⁵ L. N. Cooper, H. J. Lee, B. B. Schwartz, W. Slevart, in *Proceedings of the Eighth International Conference on Low-Temperature Physics*, London, 1962 edited by R. O. Davies (Butterworth Scientific Publications Ltd., London, 1963) p. 126.

²⁶ N. R. Werthamer, H. Suhl, T. Soda, in *Proceedings of the Eighth International Conference on Low-Temperature Physics*, London, 1962, edited by R. O. Davies (Butterworth Scientific Publications Ltd., London, 1963), p. 140.

²⁷ R. Balian and N. R. Werthamer, Phys. Rev. **131**, 1553 (1963).

²⁸ I. A. Privorotskii, Zh. Exprim. i Teor. Fiz. **45**, 1961 (1963) [English transl.: Soviet Phys.—JETP **18**, 1346 (1964)].

²⁹ A. M. Clogston, A. C. Gossard, V. Jaccarino, Y. Yafer, Rev. Mod. Phys. **36**, 170 (1964).

³⁰ R. J. Noer and W. D. Knight, Rev. Mod. Phys. **36**, p. 177.

³¹ R. H. Hammond and G. M. Kelly, Rev. Mod. Phys. **36**, p. 185.

³² W. D. Knight, in *Nuclear Magnetic Resonance and Relaxation in Solids*, edited by L. Van Gerven (North-Holland Publishing Company, Amsterdam, 1965) p. 1.

³³ P. Fulde and K. Maki, Phys. Rev. **139**, A788 (1965).

³⁴ J. Appel, Phys. Rev. **139**, A1536 (1965).

³⁵ K. Maki and P. Fulde, Phys. Rev. **140**, A1586 (1965).

³⁶ A. J. Leggett, Phys. Rev. Letters **14**, 536 (1965).

³⁷ A. I. Larkin, Zh. Exprim. i Teor. Fiz. **48**, 232 (1965)

[English transl.: Soviet Phys.—JETP **21**, 153 (1965)].

³⁸ L. P. Gor'kov, Zh. Exprim. i Teor. Fiz. **48**, 1772 (1965)

[English transl.: Soviet Phys.—JETP **21**, 1186 (1965)].

³⁹ K. H. Bennemann, Phys. Letters **17**, 197 (1965).

⁴⁰ K. H. Bennemann, Phys. Status Solidi **10**, K123 (1965).

⁴¹ W. D. Knight, in *Proceedings of the Fourteenth Colloque Ampère* (North-Holland Publishing Company, Amsterdam, to be published).

^{41a} F. Wright, Jr., W. A. Hines and W. D. Knight, Phys. Rev. Letters **18**, 114 (1967).

⁴² R. H. Hammond and G. M. Kelly, Phys. Rev. Letters **18**, 156 (1967).

^{42a} W. A. Hines and W. D. Knight, Phys. Rev. Letters **18**, 341 (1967).

⁴³ J. Bardeen, L. J. Cooper, and J. R. Schrieffer, Phys. Rev. **106**, 162 (1957); **108**, 1175 (1957).

one dimension on the order of several hundred angstroms must be used in order that the magnetic field necessary for a nuclear magnetic resonance (NMR) experiment may penetrate. In order to test this theory we have constructed a series of samples containing different sized particles of Sn metal, and measured $K(0)/K(T_c)$ for each sample. We find that $K(0)/K(T_c)$ is dependent on particle size, and the results of our experiment together with the new results on tin alloys,^{41a} on aluminum⁴² and on lead^{42a} offer very strong support for the spin-reversing scattering theory. Another theoretically proposed explanation, that some contributions to the shift would remain unchanged in the superconducting state, has been found experimentally to be unimportant.

II. EQUIPMENT AND PROCEDURES

A. Sample Production

Most of the samples were prepared in a vacuum evaporation apparatus which was an improved version of that described by Androes *et al.*⁴⁴ It consisted of a metal bell jar evacuated with an oil diffusion pump through a liquid-nitrogen trap to a pressure of about 2×10^{-6} Torr. The metal was evaporated from a resistance-heated, tungsten boat. This boat could be reloaded under vacuum by a chopping mechanism which cut 2 mm lengths of 0.038 in. tin wire and deposited them through a movable spout. The substrate was 0.00025 in. Mylar film, which could be moved under vacuum by rolling it from a supply spool over the backing plate to a take-up spool, much the same as is done with photographic film in a camera. The backing plate was cooled to liquid nitrogen temperature, but the Mylar was in poor thermal contact with it and close to room temperature during evaporation. The technique of alternate evaporation of metal and insulator was used.

The use of silicon monoxide as an insulator required some modification of the system. The SiO furnace ran continually and had a door which was opened when it was desired to deposit an insulating layer. The design of the furnace was that suggested by Drumheller.⁴⁵ In order to calibrate the evaporation rate of the furnace, a crystal oscillator monitor was built. This consisted of a crystal-controlled oscillator, the crystal of which was mounted in the vacuum system near the substrate. Part of one face was exposed to the evaporated flux so that the extra mass deposited on the face changed the crystal's mechanical resonance and therefore the frequency of the oscillator. For small changes in frequency, the change is proportional to the mass depos-

ited. The oscillator circuit used was a modification of one shown in an article by Lins and Kukuk.⁴⁶

The samples consist of 50 to 200 layers of Sn particles, depending on the sample, on one 11×12 cm sheet of Mylar which was folded until its final dimensions were 1×0.5×0.5 cm. The size of the particles was controlled by varying the amount of Sn evaporated. The three main samples constructed in this manner are labeled "1", "2", and "3" corresponding to the number of tin chops used for each layer.

A number of other samples were inspected and proved to be useful in varying degrees. A sample labeled "4" was constructed with four chops per layer. Its particles were so big that the Meissner field exclusion broadened the NMR line enough to prevent any accurate measurement of the shift in the superconducting state. The label "F" (fast) refers to a two-chop sample evaporated at a fast rate. The particle size in this sample is known less accurately than the others. The sample used by Androes and Knight,^{8,16} "A", was not rerun extensively but its linewidth was checked. Sample "L" was prepared for us by Lewis and Lindquist of California Research Corporation using an entirely different process: A tin salt was impregnated on a high surface area alumina gel, then reduced by heating it in a hydrogen atmosphere. The temperature was above the melting point of tin, and small spherical particles of metal were formed. The value of the NMR linewidth in bulk tin was determined from a sample of micron-sized particles supplied by Butterworth.

B. Nuclear Magnetic Resonance

Most of the resonance experiment equipment was quite conventional. A marginal oscillator was swept in frequency. The magnetic field was supplied by a 12 in. electromagnet and modulated at 154 cps by auxiliary coils. The output of the oscillator was fed to a phase-sensitive detector and then to a Varian time-averaging computer. This last unit is a multichannel storage device, which allows one to sweep through the resonance many times, adding the result of each sweep to the sum of all the previous sweeps. Since the signal adds coherently and the noise randomly, the signal-to-noise ratio improves as the square root of the number of sweeps. This technique is described by Klein and Barton.⁴⁷ It proved especially useful on the runs at 77°K where the signal was very weak, and it was necessary to gather data for up to 36 h.

The sample was placed in a set of double glass Dewars in order to do the experiment at liquid-helium temperatures. The temperature was varied from 4.2–1.4°K by

⁴⁴ G. M. Androes, R. H. Hammond, and W. D. Knight, *Rev. Sci. Instr.* **32**, 251 (1961).

⁴⁵ C. E. Drumheller, *Transaction of the Seventh Vacuum Symposium and First International Congress*, edited by C. R. Meissner (Pergamon Press Inc, New York, 1961), p. 306.

⁴⁶ S. J. Lins and H. S. Kukuk, *Transaction of the Seventh Vacuum Symposium and First International Congress*, edited by C. R. Meissner (Pergamon Press Inc., New York, 1961) p. 333.

⁴⁷ M. P. Klein and G. W. Barton, Jr., *Rev. Sci. Instr.* **34**, 754 (1963).

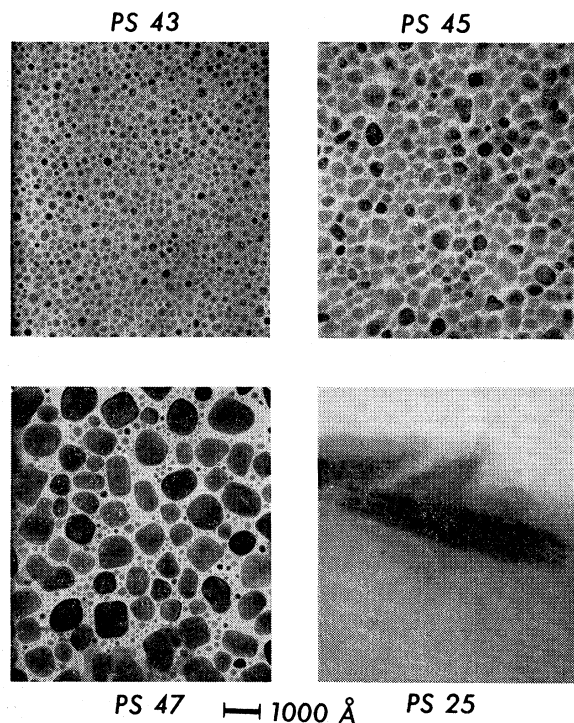


FIG. 1. Electron Micrographs of evaporated tin particles: *PS43* One chop, *PS45* Two chops, *PS47* Three chops, *PS25* Microtome sample showing three layers of two chop particles as seen edge-on.

pumping on the helium bath with a mechanical vacuum pump through a Cartesian manostat.

III. SAMPLES

A. Particle Size Determination

The particles of tin in the three main samples were in the form of platelets of diameter, d , and thickness, t . Because of the techniques involved, none of the size measurements could be made on the actual NMR samples but were made on samples evaporated under the same conditions.

Diameter. The diameter of the particles has been determined primarily by the use of an electron microscope. The samples for the electron microscope were prepared by following the procedure for making an NMR sample through the first layer, that is: a layer of SiO was deposited on the Mylar substrate; then a layer of Sn particles; then a covering layer of SiO. A 2 mm square piece of this was laid on an electron microscope grid and the Mylar dissolved off with a 3:1 mixture of trifluoroacetic acid and methylene chloride. This left a SiO film with Sn particles imbedded in it. Figure 1, *PS43*, *PS45*, and *PS47* show electron micrographs representing resonance samples "1", "2", and "3", respectively. These were taken with a Siemens Elmiskop IA at a magnification of 80 000 \times on the

original plate. Figure 2 is a histogram showing the number of particles, n , occurring at a given diameter, d , in Fig. 1, *PS43*. Because the shape of the particles is somewhat irregular, d means the diameter of a circle whose area is the same as that of the particle. Histograms from Fig. 1 *PS45* and *PS47* show similar shapes and widths, scaled to larger average size.

In determining the average size, we decided that the larger particles should count more heavily than small ones because they contribute more to the resonance intensity. One might at first conclude that the particles should be weighted according to d^3 which would be proportional to the volume if the particles had constant shape. However, it appears that the diameter grows more rapidly than the thickness as the particle grows, and that a better approximation is to assume all the particles in a given sample have the same thickness and then to weight the diameters by d^2 . Thus $\bar{d} = \frac{\sum d^3}{\sum d^2}$.

Figure 3 is a graph showing \bar{d} determined from a number of electron microscope pictures as a function of the number of chops of Sn evaporated. As one can see, the diameter of the particles is not so reproducible from run to run as one might hope. The open circles represent electron microscope samples each made on the same pump-down cycle as the corresponding NMR sample. The solid circles represent a series of samples all made during a single pump-down cycle. The solid square represents a sample evaporated at a much faster rate than the others, and illustrates that the evaporation rate has a large influence on the particle size. Since it is difficult to control the evaporation rate (the chop of metal may land in a hot or cold part of the boat and the temperature of the boat is only moderately reproducible), one can see that some variation in size is to be expected. Since we feel that there is less chance for variation in rate between evaporations made the same day as compared to evaporations separated in time by months, we chose the electron micrographs indicated by open circles in Fig. 3 as representative of NMR samples "1" and "2". The electron

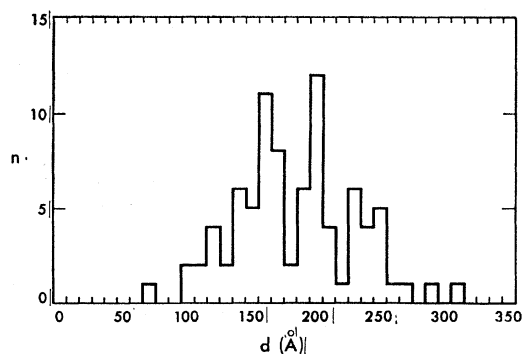


FIG. 2. Histogram of the number of particles, n , occurring at a given diameter, d , as seen in Fig. 1, *PS43*.

microscope samples closest in time to the NMR sample "3" are those of the series shown by solid circles in Fig. 3. The 570 Å (3 chop) point does not fit with the other five points of this series and is probably a fluctuation from the average. Consequently, we use the 840 Å point as characteristic of sample 3.

A summary of the data on particle diameter is contained in Table Ia. Row 1 contains the value of \bar{d} determined by the procedure indicated above. Row 2 shows the deviations of \bar{d} from the best value as indicated by the other points in Fig. 3 and indicates the possible size of fluctuations in \bar{d} . Rows 3 and 4 give some idea of the range of particle size seen in a single electron micrograph; 80% of the mass (still assuming that the thickness of all the particles is the same) occurs between the two numbers shown. A crude estimate of the particle size of an 80-layer one-chop sam-

TABLE I. Particle diameter and thickness data for the three main samples. (All values in Å)

Sample	"1"	"2"	"3"
(a)			
1. \bar{d} (best value)	200	400	840
2. deviation of \bar{d} shown in Fig. 3 from best value	+110	+220	-270
3. 90% of area above d equal	150	280	650
4. 90% of area below d equal	260	490	1070
5. \bar{d} from small angle x-rays	160
6. possible range of x-ray \bar{d}	140-210
(b)			
1. \bar{t} (best value)	130 ^a	170 ^a	260 ^b
2. range of t seen in microtome pictures	100-140	110-180	
3. deviation of \bar{t} shown in Fig. 5 from best value	-20	-10	+40
4. \bar{t} from $\cos^2\theta$ calculation]	110	160	240
5. \bar{t} from large angle x-ray line broadening	80±20		

^a From microtome pictures.

^b N/σ method.

ple was made with the aid of a small-angle x-ray scattering apparatus. The result was $\bar{d}=160$ Å (Row 5), but interpretation of the data allowed a range of values from 140 to 210 Å (Row 6).

Thickness. The electron microscope was also the primary tool used to determine the thickness of the particles. The samples for this measurement were prepared by evaporating two or three layers of Sn particles, dissolving away the Mylar substrate, potting the remaining thin film in epoxy, and, finally, sectioning it in a direction perpendicular to the plane of the film. Electron micrographs of the sections show the particles as seen edge on. Figure 1, *PS25* is an example of a picture of a three-layer, two-chop specimen. Figure 4 shows histograms for one- and two-chop samples taken from a number of pictures. Some care is needed in the

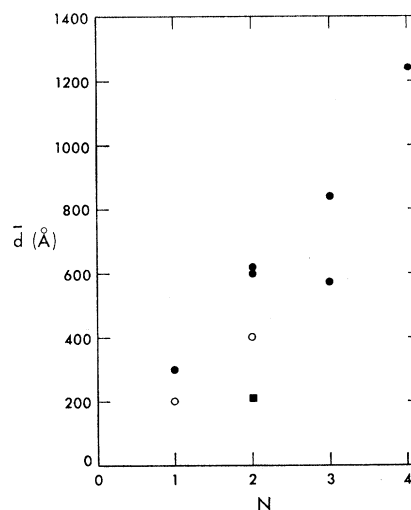


FIG. 3. Plot of the average diameter of particles, \bar{d} , as a function of the number of chops of tin evaporated, N . The solid circles represent a series of samples made during one pump-down cycle. The open circles represent samples made during the same pump-down cycle as the corresponding NMR sample. The solid square represents a sample evaporated at a fast rate.

interpretation of the pictures and histograms. The samples contain a large number of small particles which show in the pictures but represent a negligible fraction of the mass of metal. Also, in the sectioning process it is possible to cut a particle into two unequal portions. The larger portion will appear the same thickness as the whole particle would have, but the smaller portion will appear to have a small thickness. Because of these reasons we feel that the larger thicknesses shown in Fig. 4 are most representative of the samples and this fact has been taken into account in determining the "average" thickness, \bar{t} .

We were unable to obtain usable sections from samples with more than two chops of Sn per layer so another method was necessary to measure the thickness of the particles in the three-chop sample. Let us assume

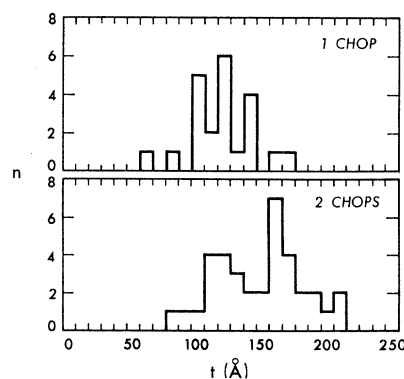


FIG. 4. Histograms of the number of particles, n , occurring at a given thickness, t , for one and two chop samples as seen in pictures like Fig. 1, *PS25*.

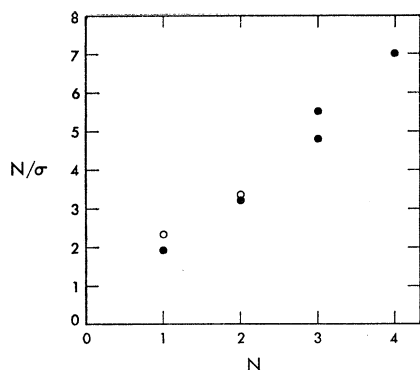


FIG. 5. Plot of the number of chops of tin evaporated, N , divided by the fraction of the area covered with particles, σ , as a function on N . The quantity N/σ should be proportional to the thickness of the particles. The same symbols are used as in Fig. 3.

as an approximation that all the particles in a sample are cylinders of variable diameter but of the same thickness, t . Then the mass of Sn per unit area of one layer, M , is equal to the fraction of the area covered with particles, σ , times the thickness, t , times the density of Sn, ρ . Solving for t we get: $t = M/\rho\sigma$. The crystal oscillator monitor has indicated that $M = M_1N$, where M_1 is the mass per unit area given by evaporating one chop and N is the number of chops actually evaporated. Thus, $t = (M_1/\rho)(N/\sigma)$. We can measure σ easily from the electron microscope pictures. Figure 5 shows a plot of N/σ (which is proportional to t) as a function of N ; the data taken from the same pictures plotted in Fig. 3. Notice particularly that there is much less variation in thickness between samples with the same N than there is in diameter. Using the value of t for the samples 1 and 2 determined from the microtome pictures, we can calculate the constant of proportionality between t and N/σ , i.e., M_1/ρ , and then use the constant to calculate t for sample 3 from its measured N/σ . The two open circles in Fig. 5 give values of M_1/ρ which differ by less than 10%. Row 1 of Table Ib gives the values of \bar{t} determined from the microtome pictures for samples 1 and 2 and determined by the method just described for sample 3. The range of thicknesses observed in the microtome pictures is indicated in Row 2. Row 3 shows the deviation of \bar{t} from the best value as indicated by the other points in Fig. 5.

One can try to evaluate M_1/ρ by a calculation involving the amount of metal evaporated. The density of Sn is 7.28 gm/cm³, and each chop weighed $9 \pm \frac{1}{2}$ mg. Assuming a $\cos^2\theta$ distribution of evaporated material we calculate the values of t shown in Row 4 of Table Ib.

Another method for determining the thickness of the particles is the broadening of large angle x-ray diffraction lines. This technique was applied to a 74 layer, one-chop sample, with the result $t = 80 \pm 20$ Å (shown in Row 5 of Table Ib). This number is slightly smaller than the values determined by other means,

but it should be noted that a number of mechanisms—strains, imperfections, and impurities—would tend to broaden the x-ray line and lead to an underestimation of t .

Other samples. Three other samples gave useful NMR results in the superconducting state, and so we should discuss the determination of their particle sizes. An electron micrograph of sample "F" showed an average diameter of 210 Å (the solid square on the graph in Fig. 3). However, an attempt to determine its thickness by the method used on sample "3" gave a number 50% larger than the diameter. We consider that this is unlikely and conclude that this method cannot be applied to samples evaporated at widely differing rates. We have no other information about t for this sample.

Androes and Knight¹⁶ quote $d = 140$ Å, $t = 40$ Å for their sample ("A"). These numbers are subject to some doubt, however. In estimating t they assumed a uniform distribution of evaporated material over a hemisphere, whereas Row 4 of Table Ib suggests that a $\cos^2\theta$ distribution is more accurate. The latter gives three times the thickness near $\theta = 0$ for a given amount of material evaporated than the former, so $t = 120$ Å is probably a better value. They also used a value of $\sigma = 75\%$ in their estimate whereas our electron microscope pictures give 50–60% as typical figures. This raises our estimate of t to 160 Å. It is more difficult to evaluate d in sample "A". Androes and Knight use only small-angle x-ray scattering to determine it. Androes mentions in his thesis that the scattering can arise from small areas of low density as well as small areas of high density so the number they get might be characteristic of the space between particles. They also observed some scattering which might arise from 210 Å diameter particles. Their small-angle x-ray results seem close to ours for sample "1". However, knowing the conditions under which "A" was evaporated, we would expect it to resemble our sample "2". Our best (but still very poor) estimate of the diameter is 300 ± 100 Å. One other piece of evidence supports the idea that the originally determined size was too small. Androes and Knight estimate that the critical field of the sample is 25 kG. Using the results of de Gennes and Tinkham⁴⁸ we find that this would correspond to a Sn sphere with $d = 250$ Å.

The size analysis on sample "L" was done by Lewis and Lindquist. Since the particles are spheres, $d = t$. From two attempts at measuring x-ray line broadening, they determined $d = 200$ and 250 Å. Electron micrographs of this sample show 600 Å diameter spheres. However, electron diffraction shows SnO₂, not Sn metal. Our interpretation of these data is as follows: just after formation, the sample consists of 600 Å spheres of Sn. In the process of transferring the sample to the x-ray apparatus, it is exposed to air and the outer part of the particles oxidizes, leaving a core of metal. The

⁴⁸ P. G. de Gennes and M. Tinkham, *Physics* **1**, 107 (1964).

200 Å run was done about three weeks after the 250 Å run so the particles were still in the process of oxidizing. Our NMR experiment on "L" was done still later so the particles might have been even smaller. We mention again, however, that there are numerous factors which tend to make this method underestimate the size.

B. Purity and Structure

After sample "2" was made, some of the evaporated material peeled from the Mylar, and this was given a semiquantitative spectrographic analysis. The results are shown below:

Mg	0.002	wt. %
Fe	<0.002	
Al	0.002	
Cu	0.001	
Ca	0.002	
Co	<0.0015	
Ni	<0.001	
Cr	<0.002	
Mn	<0.002	

This analysis includes both the metal and the insulator and indicates the sample is fairly free from metallic impurities, especially the magnetic ones, Fe, Co, Ni, Cr, Mn.

The structure of the samples was investigated with x-ray diffraction. The same x-ray lines used to determine the thickness of the 74 layer, one chop sample were used to determine its lattice constants. Because the lines are broad, the accuracy of the measurement is only fair, but we were able to notice that the (200) and (101) lattice planes both had d spacings 0.018 ± 0.009 Å too large. The measurements made by Androes and Knight on sample "A" showed the (200) planes 0.009 Å closer together than in bulk Sn.

The real problem associated with structure is that the diffraction measurements are done at room temperature whereas the resonance experiments are done at liquid-helium temperatures. The Sn particles are encased in SiO₂, which probably has a different thermal expansion coefficient from Sn. Since the sample is formed at approximately room temperature, it may be strained fairly badly when it is cooled to 4°K.

IV. THEORY

References 1-42a constitute an approximately chronological list of papers concerned with the Knight shift in superconductors. Because the list is so long, we will not discuss all of the papers but will confine ourselves to those ideas which seem most useful in interpreting our data. It is convenient to think of the total shift, K_{tot} , as made up of two parts, $K_{\text{sr}} + K_{\text{uc}}$. The shift K_{sr}

is due to the mechanism thought to be responsible for the shift in simple metals, i.e., the Fermi hyperfine contact interaction of the electron spin with the nuclear spin, where the electron spin polarization is due to a redistribution of the population of spin states in a magnetic field. The subscript sr is used because this contribution is effected by the presence of *spin-reversing* scattering as we shall see in Sec. A. Those mechanisms which remain *unchanged* through the transition to the superconduction state give rise to K_{uc} . Three of these will be discussed in Sec. B. Finally, in Sec. C, we mention certain small particle effects which one might expect to observed in NMR experiments.

A. Spin-reversing Scattering

For a qualitative discussion of this theory, the reader is referred to papers by Ferrell,⁹ Anderson,¹² and Clogston *et al.*²⁹

Anderson's treatment. Anderson¹² uses his theory for "dirty" superconductors and makes exact one-electron wave functions for the material with scattering out of plane wave states, $\psi_n = \sum_{k\sigma} \langle n | k\sigma \rangle \psi_{k\sigma}$. The matrix elements $\langle n | k\sigma \rangle$ exist because of scattering at boundaries (or impurities). The BCS formalism is now applied to these wave functions where the pairing condition of $k \uparrow$ with $-k \downarrow$ is replaced with that of n and its time reverse, \bar{n} . Because spin-orbit coupling mixes spin states, the ground state is no longer an eigenstate of spin, and therefore some polarization of the electrons is possible.

Abrikosov and Gor'kov's treatment. These authors have applied the Green's function formalism to the problem²⁴ and derive a general and precise solution. They use a scattering model based on impurity centers and say that surface scattering is equivalent, a point which remains to be proven. They also assume $l_s \gg l_r$, where l_r is the conventional mean free path which might be measured in a residual resistance experiment and l_s is the mean free path of the electron between spin flips. The most useful of their predictions is given in their equations for the case $l_s \sim \xi_0$, $T=0$.

$$K(0)/K(T_c) = 1 - \rho_0^{-1} \left[\frac{1}{2} \pi - (\cosh^{-1} \rho_0 / (\rho_0^2 - 1)^{1/2}) \right] \quad \text{for } \rho_0 > 1, \quad (3)$$

$$K(0)/K(T_c) = 1 - \rho_0^{-1} \left[\frac{1}{2} \pi - (\arccos \rho_0 / (1 - \rho_0^2)^{1/2}) \right] \quad \text{for } \rho_0 < 1, \quad (4)$$

$$\rho_0 = 2\hbar / 3\tau_s \epsilon_0 = 2\pi \xi_0 / 3l_s = 2\pi \xi_0 / 3fl_r, \quad \text{where } f = l_s / l_r.$$

A graph of this function is shown in Fig. 6. Let us see what this function implies. If the spin-orbit mean free path, fl_r , is equal to ξ_0 , then $\rho_0 \approx 2$ and $K(0)/K(T_c)$ has an intermediate value of about 0.6. If we increase the size of the particle, ρ_0 decreases and so does $K(0)/K(T_c)$, reaching a value of about 0.1 when fl_r is ten times ξ_0 . It is this limit which Yosida's calculation describes. In the opposite limit, when fl_r is one tenth of ξ_0 , $K(0)/K(T_c) \approx 0.9$.

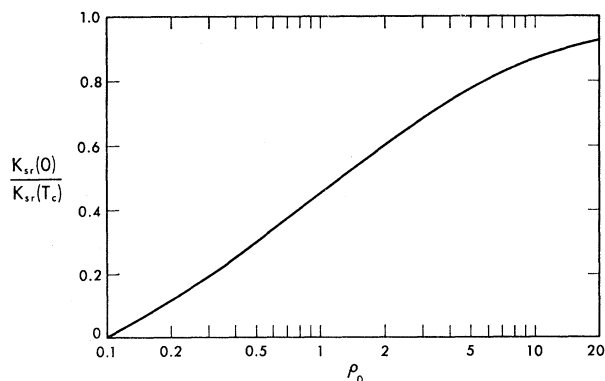


FIG. 6. Plot of the fraction of the normal state Knight shift remaining in a superconductor at zero temperature, $K_{sr}(0)/K_{sr}(T_c)$, as a function of the parameter ρ_0 . This plot refers only to that part of the shift effected by spin-reversing scattering [see Ref.24]. The quantity $\rho_0 \equiv 2\hbar/3\tau_s\epsilon_0 = 2\pi\xi_0/3fl_r$.

Appel³⁴ made a theoretical estimate of f . He finds it should be of order of $(\Delta E/\lambda)^2$, where ΔE is the gap between the conduction band and the higher band to which the orbital angular momentum connects, and λ is the spin-orbit coupling energy. For tin, using $\Delta E=3$ eV and $\lambda=0.36$ eV, he calculates $f=70$, but feels this is possibly an overestimate. It might be that ΔE is as much as a factor of 3 lower, in which case f would be about 8. In order to fit Androes's data, Ferrell estimated $f \approx 6$ and Anderson estimated $f=10-20$. Anticipating the results given in Sec. V, we note that our experiment fits theory well with f in the range of $6\frac{1}{2}-9\frac{1}{2}$.

Paramagnetic impurities. Because of the possibility of paramagnetic impurities in some of the samples used in NMR in superconductor experiments, it is useful to consider their effect on the Knight shift. Two papers, Gor'kov and Rusinov⁴⁹ and Fulde and Maki,⁵⁰ discuss conduction electron spin polarization in relation to the problem of ferromagnetism of "paramagnetic" impurities. Fulde and Maki's paper is confined to the case where l_{so} , the spin mean free path due to spin-orbit coupling, is much less than ξ_0 , that is, the case where $K(0)/K(T_c)$ is already equal to unity. This is not the situation in our samples. Gor'kov and Rusinov take into account spin-orbit effects of arbitrary size, but because the conduction electron spin polarization is only an intermediate step in their calculation, considerable work would be required to put their expressions in usable form. Lange, however, devotes a chapter of his thesis⁵¹ to the problem of the effect of magnetic impurities on the Knight shift in superconductors. He uses an approach similar to that of Abrikosov and Gorkov,²⁴ but here the flip of the conduction-electron spin occurs because of an exchange

coupling with the magnetic impurity spin instead of through spin-orbit coupling. His conclusion is contained in the following formula: $K_{sr}(0) \approx 0.18n/n_g K_{sr}(T_c)$, where n is the concentration of magnetic impurities and n_g is the concentration of magnetic impurities which reduces the superconducting energy gap to zero. In order to see a 5% change in the shift, we would have to have n/n_g equal to 0.25 which would correspond to $\frac{1}{2}$ -1% iron. This large a concentration of magnetic impurity would also produce other observable effects. The transition temperature would be lowered 10 to 20%,⁵² and the NMR line would broaden. The size of this last effect is hard to estimate, but using the data on the Cu-Mn system we conclude that the broadening might be large enough to make the line unobservable. No change in the transition temperature was detected in our samples and the line broadening we observed is not likely to be due to magnetic impurities because it is independent of temperature at low temperatures. In addition, the analysis for impurities mentioned before showed no sign of magnetic materials so we conclude that our Knight shift results are not influenced by the presence of paramagnetic impurities.

Magnetic field effects. A number of people have considered the effect of the magnetic field on $K(0)$, but it appears that these calculations are not important for our experiment. Figure 2 of the paper by Fulde and Maki³⁸ shows little change in $K(0)/K(T_c)$ for $H/H_c < 0.25$, the region in which all our experiments were done.

The predictions of the spin-reversing scattering theory, so far as our experiment is concerned, are contained in Fig. 6. The quantity f is not known very accurately and is probably best treated as an adjustable parameter, but except for this fact, there should be no problems in predicting $K_{sr}(0)/K_{sr}(T_c)$ from this graph.

B. Contributions Unaffected by the Superconducting Transition

In this section, we discuss three mechanisms which may contribute to the Knight shift but which remain unchanged when the metal goes superconducting. These are (1) Van Vleck-type orbital paramagnetism (2) Landau-Peierls diamagnetism and (3) crystalline-field spin-orbit coupling. The shifts due to these mechanisms are labeled K_{VV} , K_{LP} , and K_{cf} , respectively.

Van Vleck orbital paramagnetism. Orgel¹⁷ suggested that part of the shift, particularly in transition metals, might be associated with a Van Vleck-type, temperature-independent, orbital susceptibility, χ_{VV} . Clogston *et al.*,^{22,29} and Noer and Knight³⁰ have discussed this possibility in some superconductors. Clogston *et al.*²²

⁴⁹ L. P. Gor'kov and A. I. Rusinov, *Zh. Exptim. i Teor. Fiz.* **46**, 1363 (1964) [English transl. *Soviet Phys.—JETP* **19**, 922 (1964).]

⁵⁰ P. Fulde and K. Maki, *Phys. Rev.* **141**, 275 (1966).

⁵¹ R. V. Lange, thesis, Harvard University, 1963 (unpublished).

⁵² R. Hilsch, G. v. Minnigerode, and K. Schwidtal, in *Proceedings of the Eighth International Conference on Low Temperature Physics, London, 1963*, edited by R. O. Davies (Butterworth, Scientific Publications Ltd., London, 1963) p. 155.

give an expression relating χ_{VV} to the Knight shift: $K_{VV} = 2 \langle r^{-3} \rangle \chi_{VV} / N_0$ where $\langle r^{-3} \rangle$ is the average value of r^{-3} for p electrons in the case of Sn, χ_{VV} is expressed in emu per mole and N_0 is Avogadro's number. We can estimate $\langle r^{-3} \rangle$ by applying the Landé interval rule to the spectrum of Sn. The formulas are taken from Tinkham's group theory book,⁵³ and the energy levels from Moore.⁵⁴ The Landé interval rule is only good for light elements where spin-orbit coupling is small, and, since Sn is not light ($A=119$), we should not expect great accuracy. Indeed we find that $J=1$ and $J=2$ gives values of $\langle r^{-3} \rangle$ which differ by almost a factor of 2. The average of these two numbers is $6.4 \times 10^{25} \text{ cm}^{-3}$. We estimate χ_{VV} by partitioning the total susceptibility of Sn into several parts. $\chi_{\text{tot}} = \chi_{\text{ion}} + \chi_P + \chi_{LP} + \chi_{VV}$, where χ_{tot} is the total susceptibility, χ_{ion} is that due to the ion core, χ_P is the Pauli spin susceptibility, and χ_{LP} is the Landau-Peierls diamagnetic susceptibility. χ_{tot} is measured to be 3×10^{-6} emu/mole in Sn. χ_{ion} is calculated to be -24×10^{-6} . From the measured heat capacity $\chi_P = 23 \times 10^{-6}$. Note that we do not use the measured Knight shift to derive a value of χ_P for two reasons. First, the average shift is sensitive only to s electrons and other conduction electrons contribute to the susceptibility in Sn, and second, the whole point of this calculation is to show that the shift may be due in part to a mechanism other than the Fermi contact interaction. For free electrons $\chi_{LP} = -\frac{1}{3} \chi_P = -8 \times 10^{-6}$. This last estimate is probably the least accurate of all the numbers. The first approximation in attempting to correct the free electron value for band effects is to multiply by m/m^* . Measured values of m/m^* in Sn vary from about 0.8 to 11 depending on the direction in the crystal considered. Even this approximation is poor because it is actually possible for χ_{LP} to be positive. Adding these contributions and subtracting from χ_{tot} , we find $\chi_{VV} = 12 \times 10^{-6}$ emu/mole. Putting these numbers in our expression for K_{VV} we find $K_{VV} = 0.0026$ or $K_{VV}/K_{\text{tot}} = \frac{1}{3}$, i.e., approximately one third of the total observed shift might be associated with a Van Vleck type orbital susceptibility.

Landau-Peierls diamagnetism. We can look at the possibility of K_{LP} being important with the help of formula (12) from Noer and Knight.³⁰ With the proper values for Sn this becomes $K_{LP}/K_P \approx 1/4500 (m/m^*)^2$, where K_P is the shift associated with the Pauli spin susceptibility. Thus we see that even with m/m^* taken as ten, K_{LP} can only be 2% of K_P and is therefore not an important contribution.

Crystalline-field spin-orbit coupling. Appel suggested that crystalline-field spin-orbit coupling might account for the Knight shift observed in superconductors.³⁴ This mechanism gives a spin polarization, not through a repopulation of spin states as we discussed in spin-

reversing scattering, but through a change of polarization of the states. Since the interaction is of the high frequency or Van Vleck type, it would not be affected by the superconducting transition. The physical basis of the interaction is spin-orbit coupling of the conduction electron with the periodic electric field of the crystal. The nucleus sees this polarization through the Fermi contact interaction. Appel estimates that the ratio of the shift due to this mechanism, K_{cf} , to the total shift due to the contact interaction, K_c , is approximately equal to $\lambda/\Delta E$, where λ is the spin-orbit interaction energy and ΔE is the gap between the two bands which are connected by this Van Vleck type interaction. The quantity λ is estimated to be 0.36 eV from a calculation by Herman *et al.*,⁵⁵ on grey tin and assuming the metallic wave function is half atomic orbital, half plane wave. The quantity ΔE is chosen to be 3 eV. Then, $K_{\text{cf}}/K_c = 0.12$. As mentioned before, the value of ΔE may be up to a factor of 3 smaller so K_{cf}/K_c might be 0.36. Appel has stated that the size of the effect is probably not less than 0.12 but that the sign of the shift is uncertain.

We can see that both K_{VV} and K_{cf} may be important contributions to the shift in Sn. However, we cannot calculate either accurately enough to be able to say much further. In addition, we see no experimental way to distinguish between these two mechanisms unless the contributions to the susceptibility are understood better.

C. Small Particle Effects

We have considered three phenomena which might affect the results of an NMR experiment in small particles. Charles and Harrison⁵⁶ have written about boundary-induced charge density oscillations similar to the impurity-induced oscillations discussed by Blandin *et al.*⁵⁷ Kubo⁵⁸ and Gor'kov and Eliashberg⁵⁹ consider the effect of finite energy level spacing. Androes and Knight¹⁶ suggested a mechanism related to the anisotropic Knight shift. We have found both theoretically and experimentally that our particles are not small enough for these mechanisms to be important but that the situation might be different for particles only a factor of 2 or 4 smaller than those in sample "1".

V. RESULTS AND DISCUSSION

A. Knight Shift in Superconducting Tin

We have measured the Knight shift in samples "1", "2", and "3" as a function of temperature for several

⁵⁵ F. Herman, C. D. Kuglin, K. F. Cuff, R. L. Kortum, Phys. Rev. Letters **11**, 541 (1963).

⁵⁶ R. J. Charles and W. A. Harrison, Phys. Rev. Letters **11**, 75 (1963).

⁵⁷ A. Blandin, E. Daniel, J. Friedel, Phil. Mag. **4**, 180 (1959).

⁵⁸ R. Kubo, Phys. Letters **1**, 49 (1962); J. Phys. Soc. Japan **17**, 975 (1962).

⁵⁹ L. P. Gor'kov and G. M. Eliashberg, Zh. Exptim. i Teor. Fiz. **48**, 1407 (1965) [English transl.: Soviet Phys.—JETP **21**, 940 (1965).]

⁵³ M. Tinkham, *Group Theory and Quantum Mechanics* (McGraw-Hill Book Company, New York, 1964).

⁵⁴ C. E. Moore, *Atomic Energy Levels*, Natl. Bur. Std. (U.S.), Circ. No. 467 (U.S. Government Printing and Publishing Office, Washington D.C., 1949).

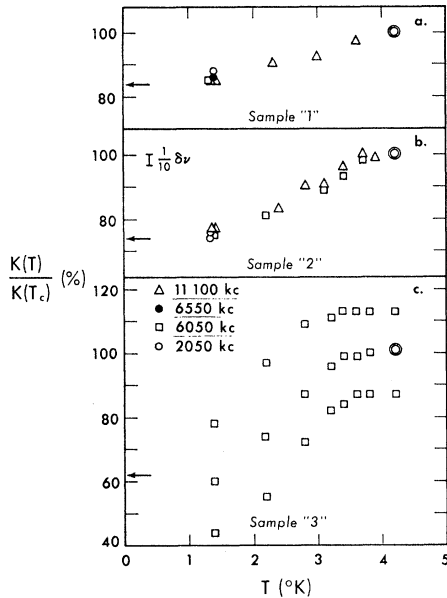


FIG. 7. Plot of the fraction of the normal state Knight shift, $K(T)/K(T_c)$, observed in three samples as a function of temperature, T . The arrows indicate the extrapolation $T=0$. The distance between the upper and lower sets of points in part *c* represents the linewidth in Sample "3" in which some Meissner broadening occurred.

values of applied field, as is shown in Fig. 7. The size of the normal state shift was arbitrarily taken to be that with reference to α tin (0.77%). The position of the line at 4.2°K was assumed to be the normal state position and all the superconducting lines are referenced to it. One tenth the linewidth was approximately 3% of the total normal state shift in all three samples (as is indicated in *b* of Fig. 7) and approximately equal to the error of the measurement of the position of the line. The transition temperature for samples "1" and "2" is 3.7°K. It is a few tenths of a degree lower for sample "3" as we can see in Fig. 7c. This drop occurs because the experiment is performed in a field of 3800 G and the critical field in sample "3" is lower than it is in the other two samples. Another consequence of the large particle size in sample "3" is that it showed some line broadening because of the Meissner effect in the superconducting state. Figure 7(c) shows three sets of points which are, from top to bottom, the position of the high frequency derivative peak, the center of the line, and the low frequency derivative peak. The vertical distance between the upper and lower sets of points represents the linewidth, which can be seen to increase by about 30% in going from 4.2 to 1.4°K. Although the Meissner broadening would tend to shift the center of the line to lower frequency, we expect it to have little effect on the position of the high frequency peak. Consequently, we can measure the change in the Knight shift by measuring the change in the position of the high frequency peak. The method used to extrapolate our

data to zero temperature was to assume that Yosida's curve remained valid with the vertical scale compressed so as to fit the data. The arrows at the left hand edge of Fig. 7 indicate this extrapolation and, in the case of sample "3", includes a small correction for Meissner broadening.

The results on four other samples should be mentioned. 1. Sample "4" showed so much Meissner broadening that it was impossible to measure the shift while it was superconducting. 2. Sample "F" gave $K(0)/K(T_c)=81\%$. 3. Sample "L" had a rather weak signal and showed some Meissner broadening but we were able to determine that $K(0)/K(T_c)=78\%$. 4. Sample "A" was not remeasured, but Andros' data will be quoted. Fitting "A" to the compressed Yosida curve we find $K(0)/K(T_c)=79\%$.

Figure 8 shows a plot of $K(0)/K(T_c)$ as a function of \bar{l} and \bar{d} for the six samples (1, 2, 3, F, L, and A) which gave useful shift results in the superconducting state. It shows the relative size and shape of the particles in the different samples. Notice particularly that the diameter of the samples 1, 2, and 3 grows more rapidly than the thickness as we mentioned in Sec. III.

In order to compare our results with theory it is necessary to estimate a value of l_r , the electronic mean free path, in our samples. The number which best represents the average dimension of the platelets is $(\bar{d}^2\bar{l})^{1/3}$. For a sphere with diffuse reflection boundary conditions, the mean free path is one half the diameter, so correspondingly, we use $\frac{1}{2}(\bar{d}^2\bar{l})^{1/3}$ as the mean free path in the particles, l . Table II gives \bar{l} and $K(0)/K(T_c)$ for the six samples. We have assumed $\bar{l}=\bar{d}$ in sample "F". The data of Table II are plotted in Fig. 9.

What can we conclude from these data? Qualitatively, $K(0)$ is a function of particle size, being larger for smaller particles, which supports the spin-reversing scattering theory. It is interesting that the data from samples "A" and "L" fit the rest of the data as well as they do because Ferrell's f factor might well have been

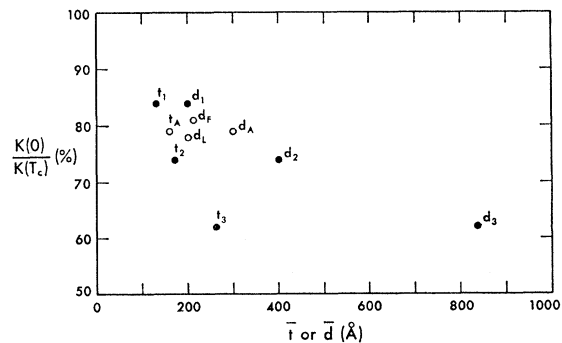


FIG. 8. Plot of the fraction of the normal state Knight shift remaining at zero temperature, $K(0)/K(T_c)$, as a function of the average diameter, \bar{d} , or thickness, \bar{l} , of the sample for the six samples, 1, 2, 3, F, L, A.

different for a Sn-nylon or Sn-SnO₂ interface than it was for a Sn-SiO interface.

We now consider quantitatively the comparison of theory and experiment, bearing in mind that the particle size data is somewhat imprecise. If K_{uc} were zero so that $K_{sr} = K_{tot}$, then we could use the observed value of $K(0)/K(T_c)$ and Fig. 6 to determine a value of ρ_0 for each sample. Since $\rho_0 = 2\pi\xi_0/3fl_r$, we would use $\xi_0 = 2000$ Å for Sn and \bar{l} for l_r and calculate an f number for each sample. Good agreement between experiment and theory would be indicated by all the f numbers being the same. However, since K_{uc} may not be zero, we should subtract K_{uc} from K_{tot} to get K_{sr} before applying the above procedure. We have tried different values of K_{uc} to find what conditions yield the most consistent set of f numbers for the samples "1", "2", and "3". For K_{uc}/K_{tot} between 0 and 20% the set of f numbers is consistent to within about 10% and f ranges from $6\frac{1}{2} - 9\frac{1}{2}$. If we try $K_{uc}/K_{tot} = 30\%$, we find a 25% range of f numbers. An attempt to fit the data to theory using \bar{l} as l_r instead of l gives a 65% range of f values for $K_{uc} = 0$ and an even wider range for all positive values of K_{uc} . We conclude that the average scattering length is related to the geometric mean of the particle dimensions rather than to the thickness of the platelets.

The linewidth in all the samples was field dependent but independent of temperature between 4.2 and 1.4°K, and approximately three times as large as the bulk value. However, runs at 77°K on samples "1", "A", and "L" showed linewidths very near the bulk value. This contradicts the theory proposed by Androes and Knight,¹⁶ and the cause of the low temperature broadening is not certain at present.

B. Related Experiments

A number of other experiments measuring the Knight shift or the conduction electron spin polarization in superconductors have been done and we will now dis-

TABLE II. Mean free path and residual shift for six samples. The error on \bar{l} cannot be represented well by a single number. One can get a more accurate picture of this error by referring to Table I for samples 1, 2, and 3 and to the section *Other Samples* in Sec. III for samples F, L, and A. The error range of $K(0)/K(T_c)$ is about 3%.

Sample	\bar{l} (Å)	$K(0)/K(T_c)$ (%)
1	85	84
2	150	74
3	285	62
F	105	81
L	100	78
A	120	79

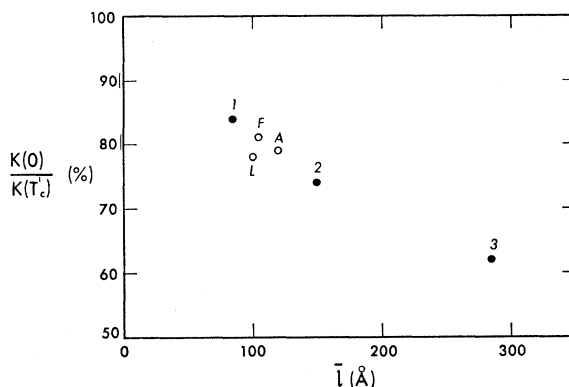


FIG. 9. Plot of the fraction of the normal state Knight shift remaining at zero temperature, $K(0)/K(T_c)$, as a function of the boundary scattering limited mean free path of the sample, \bar{l} , where $\bar{l} = \frac{1}{2}(d^2t)^{1/3}$.

cuss how they relate to our experiments and to the theories we have considered.

NMR in superconducting Hg. The first work of NMR in a superconductor was done on Hg by Reif^{1,3} and Knight *et al.*² Reif's rather careful work gave a shift at $T=0$ of 66% of the normal shift whereas Knight's preliminary result was that the shift was going towards zero as the temperature was lowered. In view of the fact that the Knight shift in the superconducting state might be a function of particle size in Hg, and that Reif's and Knight's samples did have a different range of sizes, it is not surprising that their results do not agree, although this discrepancy is large. Unfortunately, both their samples contain a rather large range of particle sizes, and most of the particles are big enough that there is appreciable Meissner broadening. Reif took the Meissner broadening into account in a rather detailed way when analyzing his data, but to take this effect and the effect of a shift varying with particle size into account at the same time when a large variation of particle size is present appears to be a formidable task. Reif's value of $K(0)/K(T_c) = 66\%$ is certainly reasonable when one considers what the spin-reversing scattering theory predicts. The spin-orbit coupling energy is only a little higher for Hg than for Sn (0.48 and 0.36 eV respectively),³⁴ but the Hg particles were somewhat larger than the Sn ones so by compensation one would expect about the same fraction of the shift to remain at $T=0$, as is observed. We have assumed in this discussion that K_{uc} is small in Hg as it is in Sn. Knight's observation of nearly zero shift in the superconducting state is difficult to understand and it would be desirable to do further experiments.

NMR in superconduction Sn. The shift results of Androes' experiment have been discussed already so we shall make only one comment here. He stated that he had observed no size dependence of the shift, having looked at a sample with 1000 Å particles as well as at "A". The measurement on the 1000 Å sample

involved the interpretation of a normal line from the bigger particles overlapping a heavily Meissner broadened superconducting line from the smaller particles. Thus, the accuracy was quite low. In addition, he was looking for a large change in $K(0)$ so we do not feel that there is any conflict between his data and ours.

NMR in superconducting Al. The third type-I superconductor to be studied was Al by Hammond and Kelly.^{31,42} This experiment was done specifically to test the spin-reversing scattering theory, Al having a small spin-orbit coupling energy of 0.022 eV. The original experiment showed the Knight shift at $T=0$ equal to 75% of the normal state value.³¹ This disagreed with the theory and was explained by saying that the films used for the experiment may have had a paramagnetic oxide layer and that an exchange interaction was reversing the spin upon scattering.³⁴ Hammond has subsequently made another sample using higher vacuum and improved evaporation techniques and has observed that the shift does go toward zero as the temperature is lowered.⁴² We note, however, that the paramagnetic oxide layer explanation does not fit well with our discussion in part IV on paramagnetic impurities. Neither the transition temperature nor the linewidth in his first sample were very different from bulk values, whereas we would expect T_c to be lower and the linewidth to be much broader if $K(0)$ is not zero.

NMR in superconducting Pb. Recent results by Hines and Knight^{42a} on small particles of Pb show results similar to those in Sn except for the f factor. For a heavy metal like Pb one would expect the large spin-orbit coupling to give rise to a small f factor and this is indeed what is observed.

NMR in superconducting Sn alloys. Some preliminary experiments by Hines^{41a} on dilute tin alloys also support the spin-reversing scattering theory. In his experiment he limits the mean free path, l_r , by adding impurities and is able to vary f by using impurities with different spin-orbit coupling strengths. For example, one atomic percent of indium produces little effect on $K(0)$ whereas the same concentration of lead raises $K(0)$ substantially.

NMR in type-II superconductors. Noer and Knight³⁰ have made a study of NMR in superconducting vanadium. The shift showed no change in the superconducting state and they concluded that most of the normal state shift was due to the rather large orbital susceptibility, which would remain unchanged in the superconducting state, and that no effects of the electron spins on the shift could be observed. This conclusion is supported by some calculations of Clogston *et al.*,²⁹ but we must remember that it is very difficult to make pure thin films of vanadium. Noer's films had a resistance ratio of only three and it is possible that impurities and lattice imperfections may have limited the spin-orbit mean free path enough to make $K_{sr}(0) \approx K_{sr}(T_c)$.

Clogston *et al.*,^{22,29} have studied V_3Si and V_3Ga . They

must do a fairly complicated analysis of their data because the shift in these metals has a large orbital contribution and a large d -band core polarization contribution. They conclude that the d electrons are superconducting and that their spin polarization drops to between 0 and 25% of the normal state value at $T=0$. This fairly complete pairing is to be expected from the spin-reversing scattering theory as they estimate $\xi_0=23 \text{ \AA}$ and $l_s > 100 \text{ \AA}$ so that $\rho_0 < 0.5$. (Polarized neutron diffraction experiments on V_3Si by Shull and Wedgwood⁶⁰ have also indicated that the V $3d$ electron spin polarization goes toward zero as the temperature goes to zero.)

Upper critical field. Strongin and Kammerer⁶¹ have measured the critical field of thin films of Al and are able to deduce information about spin polarization from these data. Clogston⁶² has pointed out that, when the magnetic field is raised to a value where $H/T_c=18\,400 \text{ G/}^\circ\text{K}$, the Zeeman energy of an electron spin, $2\mu H$, becomes equal to the superconducting energy gap, $3.5kT_c$. If the Pauli spin susceptibility, χ_P , equals zero, as in the Yosida case, then this field represents the highest possible critical field. If $\chi \neq 0$, then some alignment of the spins without the destruction of superconductivity becomes possible, and therefore the critical field may be higher. Strongin and Kammerer observe H_c values 35 to 70% higher than Clogston's limit. However, because T_c for their films is quite different from that of bulk Al and because they estimate the mean free path in their samples to be 20 \AA , it is not possible to correlate their data with the purer NMR samples of Hammond. Neuringer and Shapira⁶³ have applied the same technique to alloys of V, Nb, and Ta with Ti and find evidence of nonzero χ_P in the superconducting state.

VI. CONCLUSIONS

The theory of spin-reversing scattering is now so well supported by experiment that there is little doubt that it correctly explains $K(0)$ in tin and probably in mercury. Although we cannot rule out the possibility of an appreciable K_{uc} in Sn on theoretical grounds, experimentally it does not appear to be an important contribution. It is possible that K_{VV} and K_{ef} have opposite sign and nearly cancel one another or that our theoretical estimates of these two quantities are not accurate.

ACKNOWLEDGMENTS

The author wishes to thank a number of people for their assistance in this research project. Foremost of these is Professor Walter D. Knight who suggested the

⁶⁰ C. G. Shull and F. A. Wedgwood, Phys. Rev. Letters **16**, 513 (1966).

⁶¹ M. Strongin and O. F. Kammerer, Phys. Rev. Letters **16**, 456 (1966); **16**, 675 (1966).

⁶² A. M. Clogston, Phys. Rev. Letters **9**, 266 (1962).

⁶³ L. J. Neuringer and Y. Shapira, Phys. Rev. Letters **17**, 81 (1966).

project and gave advice and encouragement throughout its duration. Thanks are also due to the members of Professor Knight's research group, particularly Richard Noer and William Hines. Dr. Gareth Thomas allowed me to use his electron microscope and Larry Ernst instructed me in its use. Dr. James McAlear made available the ultramicrotome with which samples were sectioned, and my success with this instrument was due to the patience and guidance of Paula Finch and Ann Boardman. I was assisted in a small-angle x-ray

scattering experiment through the availability of equipment and instruction by Professor Robert Wilde and Professor Robert Hewitt of the University of California at Riverside. George Gordon performed the large angle x-ray diffraction experiments for me. Dr. Robert Lindquist and Dr. Robert Lewis of the California Research Corporation gave a great deal of time and effort to produce Sample "L". Finally, it is a pleasure to acknowledge helpful discussions with Dr. James Garland, Dr. Joachim Appel, and Dr. Robert Hammond.

Motion of Magnetic Flux through Superconducting Strips*

W. V. HOUSTON AND D. R. SMITH

Rice University, Houston, Texas

(Received 26 June 1967)

A torsion pendulum was used to measure mechanically the energy dissipation occurring in strips and vacuum-deposited films of indium as a function of the velocity with which they moved through a magnetic field normal to their surfaces. No dissipation was observed either above or below T_c when the strips moved through a uniform field. Below T_c , energy dissipation occurred in both the strips and the films when they moved through localized fields, and it was an order of magnitude greater than in the normal state. The energy loss below T_c contains a part proportional to the velocity and a velocity-independent part. An analysis of the velocity-dependent part of the losses indicates good agreement with the theoretical considerations of Bardeen and Stephen.

INTRODUCTION

IN recent years, numerous experiments¹⁻⁴ on the electrical resistance of superconducting strips in a magnetic field have been interpreted in terms of a motion of the magnetic field lines in a direction perpendicular to their length and somewhat perpendicular to the current. This motion is understood to be opposed by a constant force associated with the pinning of magnetic flux to pinning centers of an undetermined nature, plus a viscous resistance proportional to the velocity. Since all of these reported experimental results have been electrical measurements, and the motion of the flux lines has been only postulated to explain them, it seemed worthwhile to undertake a series of experiments in which the flux motion is mechanically induced. This paper is a report of one such set of measurements which shows both types of force postulated and shows a viscous force close to that calculated by Bardeen and Stephen.⁵

The experiment consisted in mounting two strips of indium radially on a phenolic disc $2\frac{1}{8}$ in. in diam. The disc was mounted as a torsion pendulum in a helium Dewar. Two pendulums were used. The periods of 23.0 and 19.6 sec were similar but the moments of inertia and the torsion constants were quite different. Two magnets, wound on nonmagnetic (glass) cores with superconducting wire, were then arranged as shown in Fig. 1 to provide a concentrated magnetic field through which the superconducting strips moved as the pendulum swung. The endpoints of each swing were observed so that the loss of energy could be determined from the difference in the squares of the endpoints and the value of the torsion constant.

It would be desirable, or course, to have a sharply discontinuous field, but in the absence of that possibility the field intensity $H(r)$ in the gap was measured as a function of the distance r from the center and could be well represented by $H(r) = H_0 \exp(-\alpha r^2)$, with $\alpha = 3.81 \text{ cm}^{-2}$. This approximate form was then used in the analysis because of its mathematical convenience.

Four different pairs of strips were used. Two were evaporated films $\frac{7}{8}$ in. long by $\frac{1}{8}$ in. wide. They were estimated to be respectively 10^8 and 8.5×10^8 Å thick, but the estimates may be in error by as much as a factor of 2. Two thicker strips were cut from sheet and were 0.0127 and 0.0508 cm thick, respectively.

* Supported in part by a grant from the National Aeronautics and Space Administration.

¹ C. F. Hempstead and Y. B. Kim, *Phys. Rev. Letters* **12**, 145 (1964).

² Y. B. Kim, C. F. Hempstead, and A. R. Strnad, *Phys. Rev. Letters* **13**, 794 (1964); *Phys. Rev.* **139**, A1163 (1965).

³ I. Giaever, *Phys. Rev. Letters* **15**, 825 (1965).

⁴ P. R. Solomon, *Phys. Rev. Letters* **16**, 50 (1966).

⁵ M. J. Stephen and J. Bardeen, *Phys. Rev. Letters* **14**, 112 (1965).

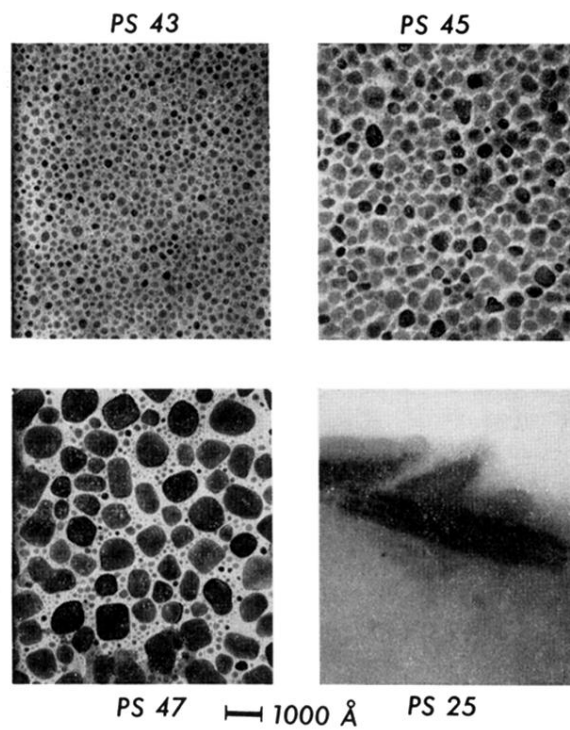


FIG. 1. Electron Micrographs of evaporated tin particles: *PS43* One chop, *PS45* Two chops, *PS47* Three chops, *PS25* Microtome sample showing three layers of two chop particles as seen edge-on.